

[2009]This manuscript version is made available under the CC-BY-NC-ND 4.0 license <http://creativecommons.org/licenses/by-nc-nd/4.0/>
This document is the Accepted Manuscript version of a Published Work that appeared in final form in Geomorphology. To access the final edited and published work see [10.1016/j.geomorph.2008.08.017]

1 **Internal structure of the aeolian sand dunes of El Fangar spit, Ebro Delta**
2 **(Tarragona, Spain)**

3

4 Rodríguez Santalla, Inmaculada^{1*}, Sánchez García, María José¹, Montoya Montes,
5 Isabel¹, Gómez Ortiz, David¹, Martín Crespo, David¹, Serra Raventos, Jordi².

6 ¹*Área de Geología, Dpto. de Biología y Geología, ESCET, Universidad Rey Juan*
7 *Carlos, C/Tulipán s/n, 28933 Móstoles (Madrid), Spain.*

8 ²*University of Barcelona, Faculty of Geology. C/ Martí i Franquès s/n, E-08028*
9 *Barcelona Spain. jordi.serra@ub.edu*

10 * Corresponding author

11 E-mail: inmaculada.rodriguez@urjc.es

12 Tel.: +34 91 488 70 17

13 Fax: +34 91 664 74 90

14

15

16 **Abstract**

17

18 This paper presents an analysis of the dune field dynamics of El Fangar Spit in the Ebro
19 Delta (Spain), associating it with the internal structure of dunes carried out with ground-
20 penetrating radar and supported by data from topographic DGPS. These analyses are of
21 great importance to ascertain the state of the internal structure of dunes as an important
22 element in their stability and, therefore in their evolution. The internal structure shows
23 accretion and progradation sequences of dunes over beach deposits, which depend on
24 dune morphology (height, crest orientation) and location, as well as the processes acting
25 on them.

26

27 **Keywords:** Ground penetrating radar, coastal dune, Ebro River Delta.

28 **1. Introduction**

29 Dunes are characteristic elements of sandy beaches in which there is great sediment
30 availability. The dunes have importance from an ecological point of view, creating their
31 own ecosystems, as well as a sediment reservoir available in times of adverse weather
32 (Houston et al., 2001). The dune field constitutes a natural coastal defence, representing
33 the main sand reserve for stormy weather. During winter the dunes are eroded by local
34 storms, carrying sand offshore where it is temporarily stored in submerged sand bars
35 forming the winter profile, thus diminishing the energy of the surge. In summer, the
36 swell transports sand bars onto the shoreline building up the beach and the dunes are
37 reconstituted again (Eisma, 1995; Charlier and de Meyer, 1998). Recognizing the
38 importance of dune performance during storms, coastal engineers have developed a
39 variety of numerical models for cross-shore sediment transport and dune erosion, a
40 review of which is given Judge et al. (2003).

41
42 The dunes represent one of the elements that have suffered considerable destruction,
43 mainly due to the massive human occupation of the coast, causing the erosion of many
44 coastal zones (Nordstrom, 2000). At present, because of the concern about the effects of
45 the climate change, and in particular the effect that the increase of sea level can cause in
46 coastal zones, there is a tendency to regenerate dunes in the places where they have
47 disappeared; this being the best mechanism of defence and conservation of beaches
48 (Hesp, 2007; Tsoar and Blumberg, 2007). Therefore, studies of the structure, behaviour
49 and evolution of dunes in different regional geographic settings are necessary.

50

51 Characteristics of dune ecosystems are conditioned by sedimentary dynamics and these
52 are mostly determined by wind field and sediment properties. For this reason it is

53 necessary to understand the internal structure of dunes in order to establish an
54 evolutionary model, which will forecast the future of the dune system. It will then be
55 possible to determine the control measures necessary to decrease dune erosion and
56 contribute to the establishment of a sustainable management plan in the Ebro Delta
57 (Sánchez et al., 2004). An understanding of dune history can assist management
58 decisions of coastal dune lands by national and state park organisations, municipalities,
59 and private landowners (Havholm et al., 2004).

60
61 Different methodologies have been used to determine aeolian dynamics such as aeolian
62 sediment traps, anemometer towers, Digital Elevation Models from different years or
63 months; but Ground Penetrating Radar offers the possibility to analyse dune evolution
64 over the long term through revealing internal dune structure.

65
66 Ground penetrating radar (GPR) is a geophysical technique used to analyse the internal
67 and geometric structures of sedimentary deposits (Bristow et al., 2000, 2005; Guha,
68 2004; Neal, 2004; Pedersen and Clemmensen, 2005; Costas et al., 2006; Aagaard et al.,
69 2007). The high resistivity of aeolian sands facilitates the penetration of the
70 electromagnetic waves emitted by GPR, favouring observation of the sedimentary
71 structures and the geometry of dunes (Moura et al., 2006).

72
73 While the dynamics of El Fangar spit have been widely studied (Maldonado, 1972;
74 Jiménez et al., 1993, 1997; Rodríguez, 1999, 2000; Rodríguez et al., 2003), research has
75 hardly gone into depth with respect to the aeolian mechanisms, although some work has
76 been completed on aeolian transport from theoretical equations (Guillén, 1992, CEDEX,

77 1996, Serra et al., 1998) that reveals its importance and its role in the processes which
78 control the deltaic evolution.

79

80 **2. Regional setting**

81 El Fangar spit is located in the north-hemidelta of the Ebro River, in Tarragona on the
82 Mediterranean coast, 170 km from Barcelona (Fig. 1). It is 2-km long sand spit with a
83 maximum width of 1.4 km at its centre, which spreads to the northwest forming a bay.
84 The inner coast of the bay presents a smooth slope easily overrun by seawater during
85 episodic storm surges.

86

87 [FIGURE 1]

88

89 The formation of the Peninsula of El Fangar is principally due to transport and
90 sedimentation of eroded material from old deltaic lobules, forming bars and beach
91 ridges parallel to the coastline (Maldonado, 1972). The spit evolution shows significant
92 accretion at its end, and it turns towards the continental coast progressively closing the
93 bay (Fig. 2). The environment is micro-tidal, with an spring tidal range of 25 cm. The
94 average offshore significant wave height (H_s) is 0.7 m, and the mean wave period (T_m)
95 is 3.9 s (Jiménez et al., 1997). The eastern wave component, the higher and more
96 energetic waves, are the predominant cause of morphological changes (Jiménez et al.,
97 1993).

98

99 El Fangar spit morphology reveals evidence of continuous reshaping. It shows two
100 different tendencies: the middle-south, joined to the deltaic body, exhibiting continued
101 erosion, while the middle-north exhibits considerable accretion (Fig. 2). The evolution

102 of El Fangar spit has been widely studied by Rodríguez (1999, 2000), and the principal
103 conclusions are: (i) the shoreline regressions are produced due to the direct coastal
104 incidence of easterly waves, and their limits are in the middle of the outer coast of El
105 Fangar spit. At this point of null movement, the coastal orientation changes, also
106 changing the evolutionary trend towards the area where the amount of sediment
107 increases, building El Fangar Spit; (ii) the width at the beginning of El Fangar Spit is
108 maintained; (iii) the bar tip has increased by 1280 m from 1957 to 2000, which
109 represents an increase of 31 m/year; (iv) the increase of the area exceeds 180 ha,
110 representing an increase rate of 4.3 ha/year. Taking into account the advance of the bar
111 tip, if the hydrodynamic conditions permit, and considering a linear tendency, it has
112 been estimated that the bay could be closed by approximately 2030.

113

114 [FIGURE 2]

115

116 The outer coast of the Peninsula of Fangar has a 6km-long dune system which
117 represents the longest and the only active dune system of the Ebro Delta (Serra, 1998;
118 Rodríguez et al., 2003). This provides a perfect nesting place for the bird life which
119 colonizes the dune field in the spring and summer seasons (Rodríguez, 2000; Sánchez et
120 al., 2004). The dune morphology is barchan type. Dune formation in the north hemidelta
121 is related to the orientation of the coast, and to the predominant wind direction of
122 greater intensity and frequency, coming from 315° (Fig. 3). The sand of the dunes
123 extends from accretion areas to the end of the spit. Its exhibits a seasonality, where El
124 Fangar spit is practically flooded by wave storms, seriously affecting the dunes, to be
125 regenerated again by returning to its initial state in calm conditions.

126

127 [FIGURE 3]

128

129 The aeolian dynamic in the study area are determined by northerly winds. Various
130 works in which the aeolian transport have been calculated from theoretical equations
131 have been carried out (Guillén, 1992; CEDEX, 1996). All of them agree that the
132 predominant direction of the aeolian transport is towards the SE, although the
133 magnitude of the transport varies substantially between authors. Serra et al. (1998) used
134 sediment traps concluding that aeolian transport is assessed at $40 \text{ m}^3/\text{m}/\text{year}$ and in
135 exceptional conditions even more. The average width of current dune field is 250 m; the
136 aeolian transport adds $10\,000 \text{ m}^3/\text{year}$ to the sediment flux of the north hemidelta
137 towards the SE. This value is almost a third of the drift transport towards the NW (Serra
138 et al., 1998).

139

140 Considering the shape and average height of the dunes, which have been monitored by
141 topographic surveys since 2005, it is possible to divide the dune field into four different
142 areas (Sánchez et al., 2007) (Fig. 4): Zone 1, is located to the north, just where the bar
143 dynamics change from an erosive to accretion tendency. It has the greatest activity, and
144 has small isolated barchans with an average height of 1 to 2 meters; Zones 2 and 3, in
145 the intermediate area, have lesser activity than zone 1 but the dunes of Zone 2 form
146 barchanoid ridges, reaching of an average height of 2 – 3 meters, and in Zone 3 the
147 shape oscillates between barchanoid and seif dunes increasing in height up to five
148 metres; Zone 4, is similar to Zone 1, but has less aeolian activity where the dune
149 morphology is barchan and the average height is 2.5 meters. Pye and Tsaoar (1990)
150 related these morphological changes to an increase in the sediment supply.

151

152 [FIGURE 4]

153

154 **3. Materials and methods**

155 As has been explained previously, the dune field of Fangar is being monitored by
156 topographic surveys with Differential Global Positioning System (DGPS), seven having
157 been completed between 2005 April and September of 2006. DGPS technology allows
158 precision in position and elevation data to less than 10 centimetres. To obtain the
159 topography with DGPS, two receptors are necessary, collecting data simultaneously.
160 One of them remained at a point of known coordinates, and the other was carried in a
161 backpack through the dune field. In this study, a topographic survey was carried out
162 synchronizing with the acquisition GPR data.

163

164 To increase the knowledge of dune dynamics at El Fangar, a study of the internal
165 structure has been performed by GPR survey. The method has been extensively used to
166 analyse the internal and geometric structures of coastal dunes (Harari, 1996; Bristow et
167 al., 2000, 2005; Van Dam et al, 2003; Pedersen and Clemmensen, 2005; Costas et al.,
168 2006, Moura et al., 2006). Considering that the Ebro Delta is a protected area, this
169 technique is especially useful due to its non-invasive character, avoiding environmental
170 damage in very sensitive areas (Bristow et al., 2000; Havholm, et al., 2004; Girardi,
171 2005) in comparison with other techniques that use trenches to study internal structures
172 (Girardi, 2005; Horwitz and Wang, 2005).

173

174 The GPR technique is based on the measurements of the subsurface response to high
175 frequency (typically 100-1000 MHz) electromagnetic (EM) waves. A transmitting
176 antenna on the ground surface emits EM waves in distinct pulses into the ground that

177 propagate, reflect and/or diffract at interfaces where the dielectric permittivity of the
178 subsurface changes. EM wave velocity data thus allow conversion of a time record of
179 reflections into an estimated depth.

180

181 Reflections of EM waves are usually generated by changes in the electrical properties of
182 sediments, variations in water content, and changes in bulk density at stratigraphic
183 interfaces. Reflections can also be related to changes in EM wave velocity due, for
184 instance, to the occurrence of voids in the ground. The penetration depth and resolution
185 of the reflection data are both functions of wavelength and dielectric constant values,
186 which in turn are mainly controlled by the water content of the materials (Daniels, 1996;
187 Davis and Annan, 1989).

188

189 Data from this study were collected with the Subsurface Interface Radar (SIR) 3000
190 system developed by Geophysical Survey Systems, Inc. (GSSI). GPR measurements
191 were made using a 200 MHz centre frequency shielded antenna in the monostatic mode,
192 which is considered the best compromise between penetration depth and event
193 resolution in sedimentary materials. All the profiles have been collected in a continuous
194 mode with a distance interval between traces of 0.1 m and a total number of 1024
195 samples per scan. In this continuous acquisition mode, each trace of the radargram is the
196 result of a 64-times stacking in order to improve the signal-to-noise ratio. A survey
197 wheel attachment was used in order to obtain a measurement at exact distance intervals,
198 in this case every 0.1 m. Thus, using the survey wheel we can be confident that the
199 accuracy in the horizontal resolution of the survey is enhanced. Automatic gain control
200 was employed during data acquisition and depending on the dune height, a time window
201 of 50 or 100 ns two way travel time (TWT) was applied. The topography along the

202 profile was obtained by means of a differential GPS and the data were used to correct
203 the topography in the data processing.

204

205 Following the scheme proposed by Neal (2004), data processing comprised zero-time
206 corrections, signal-saturation corrections, automatic gain control (AGC), band-pass
207 filtering, static corrections and Kirchoff migration. Although published data for EM
208 wave velocities in sedimentary materials are available, each specific study area displays
209 particular dielectric features due to the inherent heterogeneities of any individual
210 lithology, mostly in sedimentary rocks. For this reason, calibration surveys were
211 necessary to obtain a mean EM velocity value applicable to all profiles so that a
212 representative dielectric constant could be calculated. A calibration survey was carried
213 out over a representative zone of the area, where a metallic bar had been horizontally
214 introduced. Once the velocity data were obtained, a migration process was applied in
215 order to collapse the diffraction hyperbolae and obtain true geometries and depths of the
216 subsurface structures along the profiles. All data were processed, modelled and
217 interpreted using REFLEXW 3.5 software. In all the profiles, the position of the
218 antennae is represented on the horizontal axis, whereas depth is depicted with no scale
219 exaggeration on the vertical.

220

221 As a general statement, GPR profiles exhibit a good signal-to-noise ratio over the whole
222 time window. In addition to this, all GPR profiles show a much higher intensity at the
223 central part, corresponding to the coastal dunes, than at the edges, where water-saturated
224 sands are predominant. Moreover, a reflector located at a constant depth of about 0.7 m
225 below the plain can be seen in all the profiles, although under the dune formations it is
226 obscured by other reflectors. From direct field observations made at small trenches, the

227 0.7 m depth reflector closely matches the location of the water table. Conductive saline
228 groundwater increases attenuation below the water table, as well as introducing
229 interferences in the GPR diagrams, especially if the pores are filled with salt water. This
230 would be the cause of some persistent repetitions of parallel reflectors present in the
231 lower part of the records, in addition to deeper reflections that could be multiples of the
232 air and ground waves at the top of the profile. For these reasons, the profiles have not
233 been interpreted below the water table except where attenuation is low.

234

235 During the field survey, 14 GPR profiles with a total length of 1120 m were carried out.
236 The location of the profiles was planned according to the different zones of dune
237 activity. This paper shows only 5 profiles (Fig. 4) chosen from 14 GPR profiles, to
238 explain the internal structure of the dune field at El Fangar Spit.

239

240 In addition, to understand the present aeolian dynamics the monthly wind roses from
241 April to September of 2006 (Fig. 5), as well as the wave roses (Fig. 6) and the sea-level
242 variations (Fig. 7) for the same period have been analyzed. All these data have been
243 made available by the Red de Instrumentos Oceanográficos y Meteorológicos (XIOM)
244 of Generalidad de Cataluña. The meteorological station is located in the Port of
245 L'Ampolla about 6 km from the El Fangar dune field. The data are provided for every
246 10 minutes. Fig. 5 shows monthly wind roses from April to September of 2006, which
247 reflect wind direction changes in the months of summer. The wave roses in Fig. 6
248 present the hourly significant heights of the waves. The buoy is directional, anchored in
249 the Cabo de Tortosa approximately one km from the El Fangar coast. The tide-gauge
250 data are correlated with the same time period of the meteorological station.

251

252 [FIGURE 5]

253 [FIGURE 6]

254 [FIGURE 7]

255

256 **4. Results**

257 **4.1 Topographic surveys**

258 From topographic surveys with DGPS, different Digital Elevation Models (DEM) have
259 been obtained, which have been used to estimate field dune movement (Fig. 8).

260 Migration rates were calculated between each survey by superposition of MDT with a
261 Geographic Information System (GIS). The method used can be seen in Sánchez et al.
262 (2007).

263

264 [FIGURE 8]

265

266 **4.2 Ground Penetrating Radar survey**

267 To explain the internal structure of the dunes a profile from the GPR survey in each
268 zone is shown (Fig. 4).

269 **4.2.1 Zone 1**

270 Profile 1 (Fig. 9) was acquired in zone 1, parallel to the prevailing wind direction and
271 parallel to the shoreline, cutting two barchan type dunes lengthwise. In this profile, the
272 reflectors are parallel and sub-horizontal by foreset accretion. At a horizontal distance
273 of between 10 and 20 m, truncations in the radargram sequence can be observed. In the
274 interdune zone (20 – 30 m distance), the reflectors are sub-horizontal, showing vertical
275 accretion. From 38 m there are onlap relations associated with dune migration towards
276 the SE.

277

278 [FIGURE 9]

279

280 Profile 2 (Fig. 10), is perpendicular to profile 1, perpendicular to the shoreline, and
281 parallel to the dune crest. The reflectors stay sub-horizontal, showing foreshore
282 accretion, but at 28 m and 32 m distance there are convex-up reflectors which maintain
283 onlap relations in the lateral ones, adapting to a morphology of the underlying beach,
284 represented by a continuous reflector. Over this formation dune radar facies are
285 developed showing parallel lamination.

286

287 [FIGURE 10]

288

289 **4.2.2 Zone 2**

290 Profile 3 (Fig. 11) was carried out parallel to the shoreline and predominant wind
291 direction of greater intensity. It is possible to distinguish two radar facies, separated by
292 the water table. The lower is defined by continuous low angle reflectors that correspond
293 to beach facies (Bristow et al., 2000; Bristow and Pucillo, 2006), and overlapping this is
294 another dune facies, showing discontinuous reflectors, dipping in the wind direction at a
295 low angle forming cross-stratification typical of the movements of the migration of the
296 dune. At a horizontal distance of 68 m, it is possible to distinguish a wedge geometry
297 from avalanching due to brink reactivation by the prevailing wind.

298

299 [FIGURE 11]

300

301 **4.2.3 Zone 3**

302 Zone 3 is represented by profile 4 (Fig. 12). The internal structure is similar to the
303 previous one. Below the water table, there are low-angle reflectors and parallel
304 lamination due to foreset accretion. Above the water table, the modification of wind
305 flow around the main dune body is shown by short SE-dipping reflectors forming cross-
306 stratification, which are interpreted as dune progradation (e.g. Pye and Tsoar, 1990;
307 Bristow et al., 2000; Pedersen and Clemmensen, 2005; Bistow and Pucillo, 2006). On
308 the rearslope face, there are sets of trough cross-stratification scour and fill. Also, a
309 wedge geometry at 58 m distance overlaps the previous unit.

310

311 [FIGURE 12]

312

313 **4.2.4 Zone 4**

314 Profile 5 (Fig. 13) in zone 4, was carried out over two small Barchan dunes separated by
315 an interdune depression. In general, all the units are laterally continuous and are
316 characterized by sub-horizontal reflectors. These radar facies are interpreted as
317 foreslope accretion. Onlap reflectors are found at a distance of between 30 to 40 m, and
318 70 to 80 m. In addition, a small unit of trough cross-stratification from scour and fill is
319 present in the slipface of both dunes. The presence of different partially overlapping
320 units on the dune crest is interpreted as being due to rearslope and active dune migration
321 during periods of increased sand mobility.

322 [FIGURE 13]

323

324 **4.3 Wind and Wave Roses**

325 The analysis of wind roses of April to September of 2006 (Fig. 5) shows that the main
326 wind direction has a north component, but emphasizes the change in June when there is

327 a greater wind frequency from E-ENE, with speeds greater than the speed threshold of
328 movement (4 m/s according to Serra et al., 1998). In July and August a wind storms
329 from the SW direction and with speeds greater than 10 m/s are also observed. The wave
330 roses of these months are analyzed (Fig. 6) in the same way, distinguishing two storms
331 from the E, with significant wave heights greater than 1.5 m, which agrees with the
332 surge elevations caused by meteorological tide (Fig. 7), and favouring waves of high
333 energy which affect the field dune.

334

335 **5. Discussion**

336 According to Sánchez et al. (2007), and considering the migration rates shown in Fig. 8,
337 the dune field of El Fangar spit is highly active, distinguished by different zones defined
338 by dune activity linked to coastal and aeolian processes. The internal structure reveals
339 the dynamic history of dunes. If the DEM obtained from the topographical survey with
340 DGPS in April of 2006 (Sánchez et al., 2007), and those obtained with the GPR data
341 from September of 2006 are compared, it is possible to determine that associated
342 aspects of the existing structures in each profile are derived from events that happened
343 between the dates compared (April to September 2006) using wind and wave roses
344 (Figs. 5, 6). The evolution obtained by means of topographic data shows that zones with
345 low heights have migration rates higher than zones with higher dune height. Then, to
346 explain the internal structure it is necessary to establish a relationship with the dune
347 height, suggesting that low height (zones 1 and 4) involves significant migratory
348 activity, while a height increase (zones 2 and 3) leads to a decrease in dune migration,
349 showing a more developed internal structure.

350

351 Profiles 1 and 2 are located to the north, just where the bar dynamics change from
352 erosive to accretionary tendency. It has the greatest dune activity since they are directly
353 facing north winds. In relation to profile 1 it is possible to point out that the first 14
354 meters are developed on top of that which, in the DEM of April of 2006, was occupied
355 by sand flats (Fig. 14). This can explain the different relations associated with wind
356 reactivation and the advance of dune towards the SE that are observed in zone 1 (Fig.8).
357 During months of May, July and August of 2006 episodes of southerly wind of great
358 intensity took place (Fig. 5), affecting the dune morphologies and changing the
359 direction of the crests (Fig. 15). These changes are registered in the internal structure of
360 the dunes in form of truncations like those observed between the 10 and 20 m distance
361 in profile 1.

362

363 [FIGURE 14]

364 [FIGURE 15]

365

366 Given the low height of the dune in zone 1, it is possible to distinguish in the base of the
367 radargram of profile 2 (Fig. 9) different shapes that can be explained as positive relief of
368 the beach ridges (Neal and Roberts, 2000) forming El Fangar Spit, which are covered
369 by dunes.

370

371 In comparison with zone 1, the height and complexity of the dunes increases in zone 2
372 and zone 3, which contain dunes of greater size, implying a decrease in dune migration
373 (Sánchez et al., 2007). The radar facies of both zones show structures in line with the
374 previous findings, presenting radar facies which are more continuous laterally, with low
375 angle foresets associated with dune accretion, following a normal sequence with a low

376 grade of mobility, and being more developed. The cross-stratification in the radar facies
377 of dune is interpreted as dune progradation showing different phases of dune
378 reactivation (e.g. Pye and Tsoar, 1990; Bristow et al., 2000; Pedersen and Clemmensen,
379 2005; Bistow and Pucillo, 2006). Beside this, wedge geometry overlaps the previous
380 unit with trough cross-stratification from scour and fill. This could correspond to the
381 resulting deposit from a small avalanche of the windward face of the dune due to
382 reworking by the prevailing wind (Bristow et al., 2000).

383
384 Zone 4 is located to the south of the dune field, and it exhibits smaller dunes than the
385 others. This is because the wind and the sediment, coming from the north, previously
386 feed the dune bodies of zones 1, 2 and 3. In this way, a lesser amount of sand arrives to
387 form the dunes of this zone. The radar facies on GPR profiles across the dune in zone 4
388 contain trough cross-stratification cut and fill, and roll-over structures; all of them
389 associated with active dunes, with reworking by winds. The shoreline trend is different
390 in the four areas, the erosion rate of the coastline diminishing from the south towards
391 the north (Jiménez et al., 1997; Rodríguez et al., 2003). This is also reflected in the
392 coastal orientation, so that the northern formation receives more oblique waves coming
393 from the east, zone 4 being the nearest to the coastline and more affected by waves (Fig.
394 16).

395
396 As a result the dune formation located to the south of the dune field presents greater
397 problems because of the effect of the waves, being clearly reflected in their internal
398 structure where it is possible to distinguish truncations due to erosion by wave storms
399 events (Fig.12) (Bristow and Pucillo, 2006; Costas et al., 2006; Moura et al., 2006).

400

401 [FIGURE 16]

402

403 **6. Conclusion**

404 The internal structure of dunes can be explained by the dune activity and aeolian and
405 wave dynamics. Zone 1 shows small and low dunes, but high aeolian activity because
406 they are the first to face effective winds from the NW. The internal structure of these
407 dunes shows intense migratory activity in response to wind direction, towards the SE. In
408 addition, a bar from accretion of sand that forms El Fangar Spit has been observed at the
409 base of the dune.

410

411 The intermediate area of the dune field, showing less activity than the zone 1, exhibits
412 two zones (zones 2 and 3) in line with the dune type. In both cases, the dunes are higher
413 than in other zones, and have a low migration rate. An important foreshore accretion is
414 observed in the GPR profiles, as well as superficial activity marked by cross-
415 stratification, due to wind action.

416

417 Zone 4, located to the south of the dune field, presents very small dunes. Due to its
418 position in relation to coastal orientation, they are influenced by northerly winds and
419 they are also affected by easterly waves of greater energy. These are the cause of
420 significant erosion of coastline in this zone. This activity is reflected in the dune internal
421 structure, showing different truncations by storm waves.

422

423 From the GPR data analysis it is possible to confirm that the morphology and the
424 geometry of the dune bodies adapt themselves to meteorological conditions. This allows
425 us to make an extensive study of dune activity and to obtain models of coastal dune

426 development, in order to advise on the most effective mechanisms for the management
427 and maintenance of the dune fields.

428

429 The structure of dunes is the result of the processes that occur in the zone during a short
430 period of time. Having DEMs of dunes from previous surveys, as well as data of wind
431 and waves of months previous to the acquisition of radargrams, facilitate interpretation
432 of the internal structure in relation to recent dynamics. In zones such as the Fangar Spit,
433 where during the months of April to August there is no access in order to allow the
434 nesting of birds, the GPR technique turns out to be helpful in understanding the
435 significance of dynamic processes during this period when it is not possible to study
436 dune topography directly.

437

438 **7. Acknowledgments**

439 We would like to thank of the *Parque Natural* of Ebro Delta for permitting fieldwork in
440 the area. This work is funded by the Project “Cuantificación y contribución del
441 transporte eólico en los procesos dinámicos y ambientales en el delta del Ebro.
442 Aplicación a su gestión integrada y a la conservación de los ambientes marginales”,
443 from the Ministerio de Ciencia y Tecnología of Spain. Moreover, we would like to give
444 thanks to the Red de Instrumentos Oceanográficos y Meteorológicos (Generalidad de
445 Cataluña) for the data provided.

446 **8. References**

447 Aagaard, T., Oxford J., Murray, A.S., 2007. Environmental controls on coastal dune
448 formation; Skallingen Spit, Denmark. *Geomorphology* 83, 29-47.

449

450 Bristow, C.S., Chroston, P.N., Bailey, S.D., 2000. The structure and development of
451 foredunes on a locally prograding coast: insights from ground-penetrating radar surveys,
452 Norfolk, UK. *Sedimentology* 47, 923-944.

453

454 Bristow, C.S., Lancaster, N., Duller, G.A.T., 2005. Combining ground penetrating radar
455 surveys and optical dating to determine dune migration in Namibia. *Journal of the*
456 *Geological Society, London* 162, 315-321.

457

458 Bristow, C.S., Pucillo, K., 2006. Quantifying rates of coastal progradation from
459 sediment volume using GPR and OSL: The Holocene fill of Guichen Bay, south-east
460 South Australia. *Sedimentology* 53, 769-788.

461

462 CEDEX, 1996. Estudio de la dinámica litoral del Delta del Ebro y prognosis de su
463 evolución. *Dinámica litoral del Delta del Ebro*. Centro de Estudios de Puertos y Costas,
464 CEDEX. Technical Report, Direccion General de Costas, MOPTMA, Madrid, Spain, 155
465 pp.

466

467 Costas, S., Alejo, I., Rial, F., Lorenzo, H., Nombela, M.A., 2006. Cyclical evolution of
468 a modern transgressive sand barrier in Northwestern Spain elucidated by GPR and
469 aerial photos. *Journal of Sedimentary Research* 76, 1077-1092.

470

471 Charlier, R.H., de Meyer, C.P., 1998. Coastal erosion: response and management. Ed.
472 Springer. 343 p.
473

474 Daniels, D.J., 1996. Surface-penetrating radar-IEE Radar, Sonar, Navigation and
475 Avionics Series 6: London, The Institute of Electrical Engineers, 320 p.
476

477 Davis, J.L., Annan, A. P., 1989. Ground-penetrating radar for high-resolution mapping
478 of soil and rock stratigraphy: Geophysical Prospecting 37, 531-551.

479 Eisma, D., 1995. Climate Change: Impact on Coastal Habitation. CRC Press, 272 p.
480

481 Girardi, J.D., 2005. A GPR and Mapping Study of the Evolution of an Active Parabolic
482 Dune System, Napeague, New York. PhD Thesis, Dept. of Geosciences, Stony Brook
483 University, Manhattan.
484

485 Guillén, J., 1992. Dinámica y balance sedimentario en los ambientes fluvial y litoral del
486 Delta del Ebro. PhD Thesis, Universidad Politécnica de Cataluña, Barcelona, Spain, 580
487 pp.
488

489 Guha, S., 2004. Ground penetrating radar response to thin Layers: Examples from
490 Waites Island, South Carolina. PhD Thesis, University of South Florida.
491

492 Harari, Z., 1996. Ground-penetrating radar (GPR) for imaging stratigraphic features and
493 groundwater in sand dunes. Journal of Applied Geophysics 36, 43-52.
494

495 Havholm ,K.G., Ames, D.V., Whittecar, G.R., Wenel, B.A., Riggs, S.R., Jol, H.M.,
496 Berger, G.W., Holmes, M.A., 2004. Stratigraphy of Back-Barrier Coastal Dunes,
497 Northern North Carolina and Southern Virginia. *Journal. of Coastal Research* 20-4,
498 980–999.
499
500 Hesp, P., 2007. Initiation, Evolution, Dynamics and Geomorphology of Transgressive
501 Dunefields. *International Conference on Management and Restoration of Coastal*
502 *Dunes*. Santander, Spain.
503
504 Horwitz, M., Wang, P., 2005. Sedimentological Characteristics and Internal
505 Architecture of Two Overwash Fans from Hurricanes Ivan and Jeanne. *Gulf Coast*
506 *Association of Geological Societies Transactions*, Volume 55, 342-352.
507
508 Houston, J., Edmondson, S.E., Rooney, P.J., 2001. *Coastal Dune Management: Shared*
509 *Experience of European Conservation Practice* Liverpool University Press, 458 p.
510
511 Jiménez, J.A. and Sánchez-Arcilla, A. 1993. Medium-term coastal response at the Ebro
512 Delta, Spain. *Marine Geology*, 114, 105-118.
513
514 Jiménez, J.A., Sánchez-Arcilla, A., Valdemoro, H.I., Gracia, V. and Nieto, F. 1997.
515 Processes reshaping the Ebro delta. *Marine Geology*, 144, 59-79.
516
517 Judge, E.K., Overton, M.F., Fisher, J.S. 2003 Vulnerability indicators for coastal dunes.
518 *Journal of Waterway Port Coastal and Ocean Engineering* 129 (6), 270–278.
519

520 Maldonado, A., 1972. El Delta del Ebro. Estudio sedimentológico y estratigráfico. PhD
521 Thesis. Universidad de Barcelona, Spain. Boletín de Estratigrafía, Vol. 1 486 p.
522

523 Moura, M.V.M., Reyes-Perez, Y.A., Siqueira, D., Santos, D.A., Medeiros, A., Reis,
524 A.P.M., Pinheiro, F., 2006. Levantamento geofísico com GPR em um campo de dunas
525 eólicas em Tibau do Sul/RN. Revista de Geología 19(1), 99-108.
526

527 Neal, A., Roberts, C.L., 2000. Applications of ground-penetrating radar (GPR) to
528 sedimentological, geomorphological and geoarchaeological studies in coastal
529 environments. In: Pye, K.; Allen, J.R.L. (Eds.), Coastal and estuarine environments:
530 sedimentology, geomorphology and geoarchaeology, Geological Society, London,
531 Special Publications, 175, pp. 139-171.
532

533 Neal, A., 2004. Ground-penetrating radar and its use in sedimentology: principles,
534 problems and progress. Earth-Science Reviews 66, 261-330.
535

536 Nordstrom, K.F., 2000. Beaches and Dunes of Developed Coasts. Cambridge
537 University Press. 338 p.
538

539 Pedersen, K., Clemmensen, L.B., 2005. Unveiling past aeolian landscapes: A ground-
540 penetrating radar survey of a Holocene coastal dunefield system, Thy, Denmark.
541 Sedimentary Geology 177, 57-86.
542

543 Pye, K., Tsoar, H., 1990. Aeolian Sand and Sand Dunes, Unwin Hyman, London.
544

545 Rodríguez, I., 1999. Evolución Geomorfológica del Delta del Ebro y Prognosis de su
546 Evolución. PhD Thesis, Universidad de Alcalá de Henares, Alcalá de Henares, Spain.
547

548 Rodríguez, I., 2000. Proyecto de actuación medioambiental en el entorno de la
549 Península del Fangar, Playa de la Marquesa y Playa de Pal en el Delta del Ebro. Estudio
550 de Impacto Ambiental. Technical Report, Direccion General de Costas, Ministerio de
551 Medio Ambiente, Madrid, Spain.
552

553 Rodríguez, I., Galofré, J., Montoya, F., 2003. El Fangar spit evolution. Coastal
554 Engineering VI: Computer Modelling and Experimental Measurements of Seas and
555 Coastal Regions. WIT PRESS, UK, pp. 419-425.
556

557 Sánchez, M.J., Rodríguez, I., Serra, J., 2004. Evolution of shoredune field on the Ebro
558 Delta (Spanish Mediterranean Coast). Littoral 2004, Aberdeen, Escocia, UK, pp. 719-
559 720.
560

561 Sánchez, M.J., Rodríguez, I., Montoya, I., 2007. Short term coastal dune evolution of
562 Fangar Spit (Ebro Delta, Spain). International Conference on Management and
563 Restoration of coastal dunes. Santander, Spain.
564

565 Serra, J., Maia, L.P., Bautista, R., 1998. Aeolian contribution to the sediment budget
566 along the coast of the Ebro delta. 15 th International Congress of Sedimentology.
567 Alicante, Spain.
568

569 Tsoar, H., Blumberg, D.G., 2007. Management of stable and active coastal sand dunes.
570 International Conference on Management and Restoration of coastal dunes. Santander,
571 Spain.
572
573 Van Dam, R.L., Van Den Berg, E.H., Schaap, M.G., Broekema, L.H., Schlager, W.,
574 2003. Radar reflections from sedimentary structures in the vadose zone. Geological
575 Society of London, Special Publications 211, 257-273.

ACCEPTED MANUSCRIPT

576 **Figure captions**

577 Figure 1. Location of the study area in the Iberian Peninsula.

578

579 Figure 2. Coastline variation in 40 years. Different values of erosion and accretion are
580 shown, according to Rodríguez, et al. (2003).

581

582 Figure 3. Wind rose of the delta of the Ebro, 1992-2007. Hourly data coming from the
583 Fangar weather station belonging to the Red de Instrumentos Oceanográficos y
584 Meteorológicos managed by Generalidad de Cataluña.

585

586 Figure 4. Position of profiles and dune field division (Sánchez et al., 2007).

587

588 Figure 5. Wind roses from April to September 2006. Data acquired every 10 minutes
589 coming from L'Ampolla weather station belonging to the Red de Instrumentos
590 Oceanográficos y Meteorológicos of Generalidad de Cataluña.

591

592 Figure 6. Wave roses from April 2006 to September 2006. Data acquired every hour
593 coming from Cap Tortosa directional buoy belonging to the Red de Instrumentos
594 Oceanográficos y Meteorológicos of Generalidad de Cataluña.

595

596 Figure 7. Sea-level variation from April to September 2006. Data acquired every 10
597 minutes coming from L'Ampolla tidal gauge belonging to the Red de Instrumentos
598 Oceanográficos y Meteorológicos of Generalidad de Cataluña.

599

600

601 Figure 8. Migration rates from September 2005 to September 2006, obtained by DEM
602 comparison (Sánchez et al., 2007).

603

604 Figure 9. Profile 1, parallel to wind direction. In this profile it is possible to distinguish
605 reflectors (A) parallel and sub-horizontal by foreset accretion; truncate reflectors (B)
606 associated with storm events, and in onlap relations due to dune migration towards the
607 SE.

608

609 Figure 10. Profile 2, perpendicular to profile 1. This profile presents parallel lamination
610 (A) adapting to underlying shapes which are interpreted as beach ridges (B) that form El
611 Fangar Spit.

612

613 Figure 11. Profile 3, parallel to wind direction. It is possible to distinguish the beach
614 facies (A) defined by continuous low angle reflectors, and dune facies (B) forming
615 cross-stratification dipping in the wind direction. The rearslope face presents an
616 activation wedge (C) due to an increase in the activity of the wind.

617

618 Figure 12. Profile 4, parallel to wind direction. This profile present parallel lamination
619 (A) by foreset accretion, where the dune facies are developed (B) with cross
620 stratification parallel to the wind direction. Sets of trough cross-stratification (C) are
621 present in the rearslope face, and a wedge geometry (D) caused by at deposit from a
622 small avalanche.

623

624 Figure 13. Profile 5, parallel to wind direction. Shows two dunes separated by an
625 interdune depression (A) with parallel lamination. It is possible to distinguish

626 truncations (B) associated with dune overwashing, and overlapping units (C) in the
627 rearslope face associated with dune migration.

628

629 Figure 14. Location of Profiles 1 and 2 in April 2006.

630

631 Figure 15. Barchan dunes with three brinks oriented in three different directions.

632

633 Figure 16. Inundation of the dune field during periods of storm.

ACCEPTED MANUSCRIPT

Figure 1

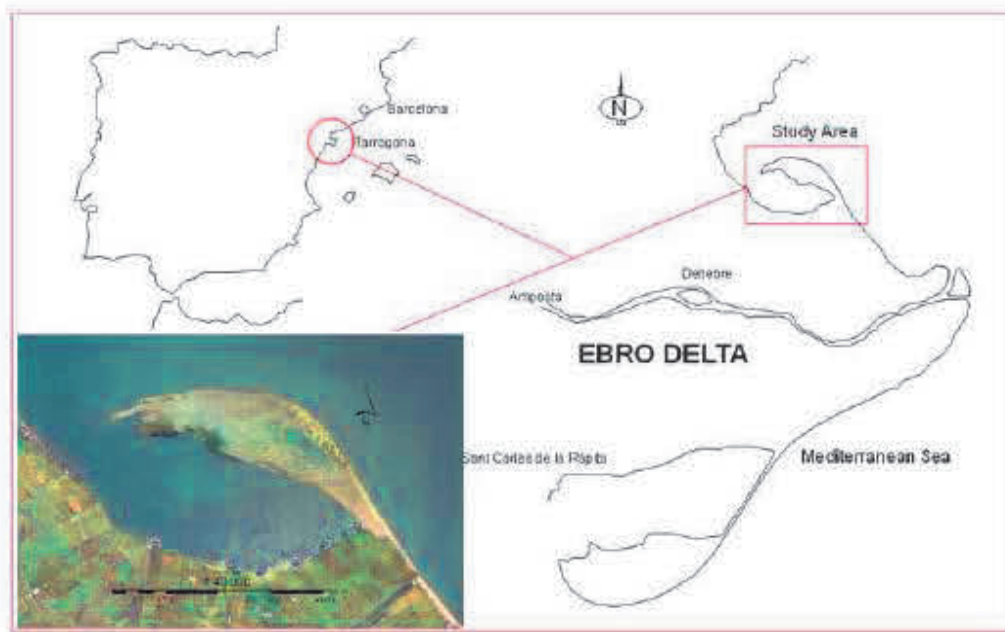
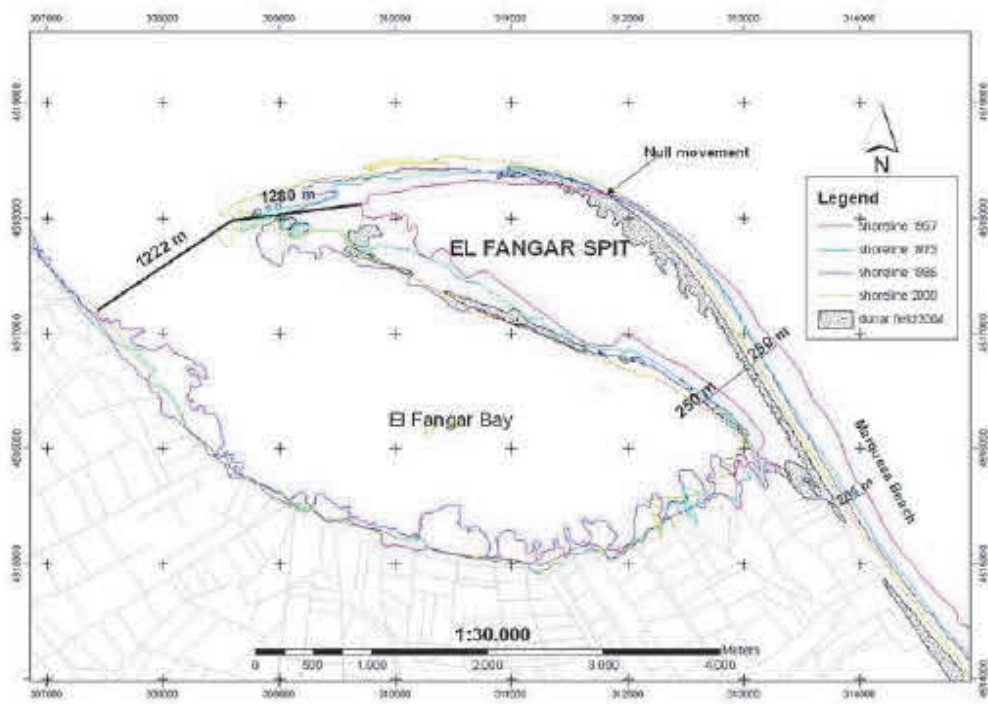


Figure 2



635

ACCEPTED

Figure 3

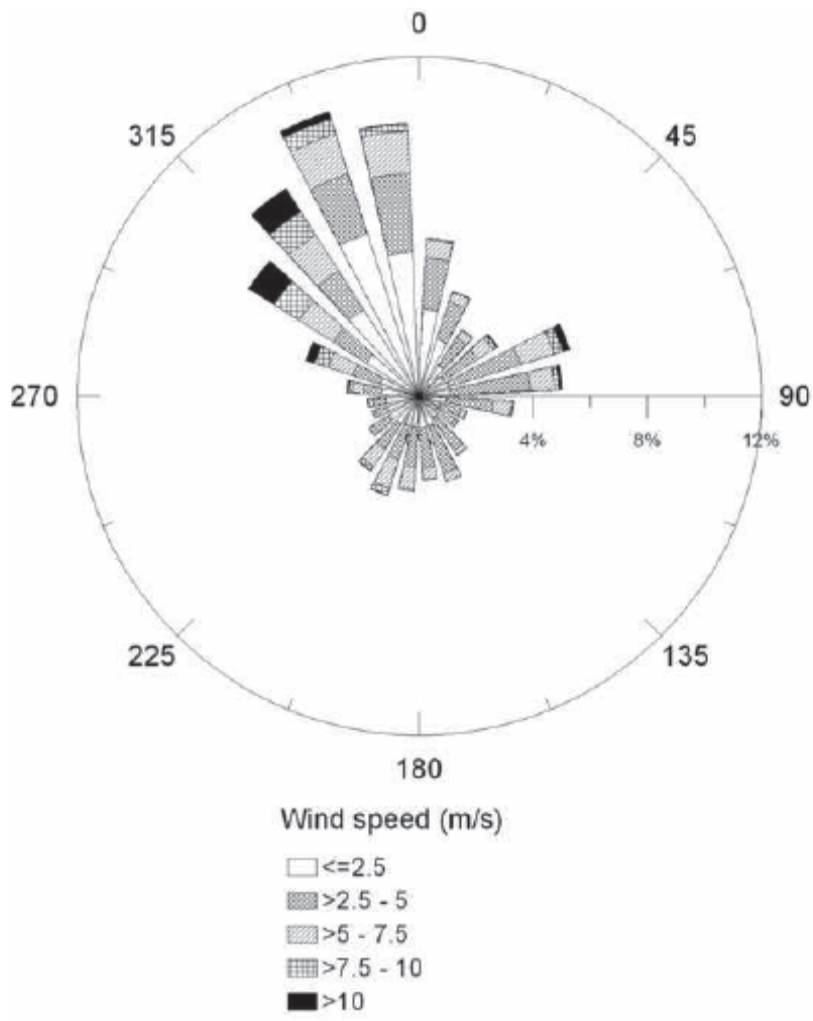


Figure 4

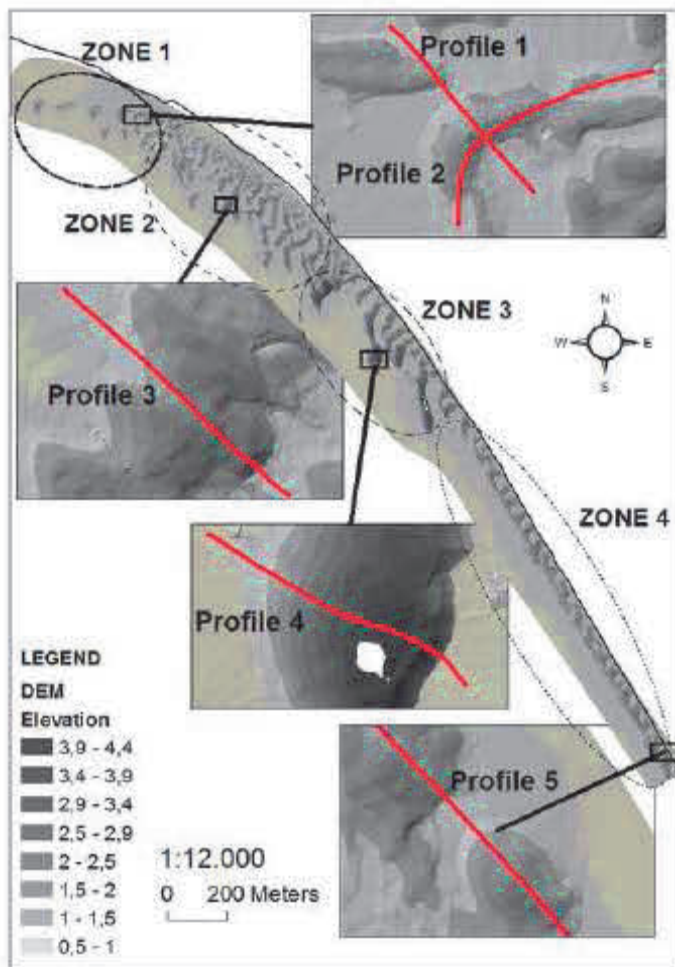


Figure 6

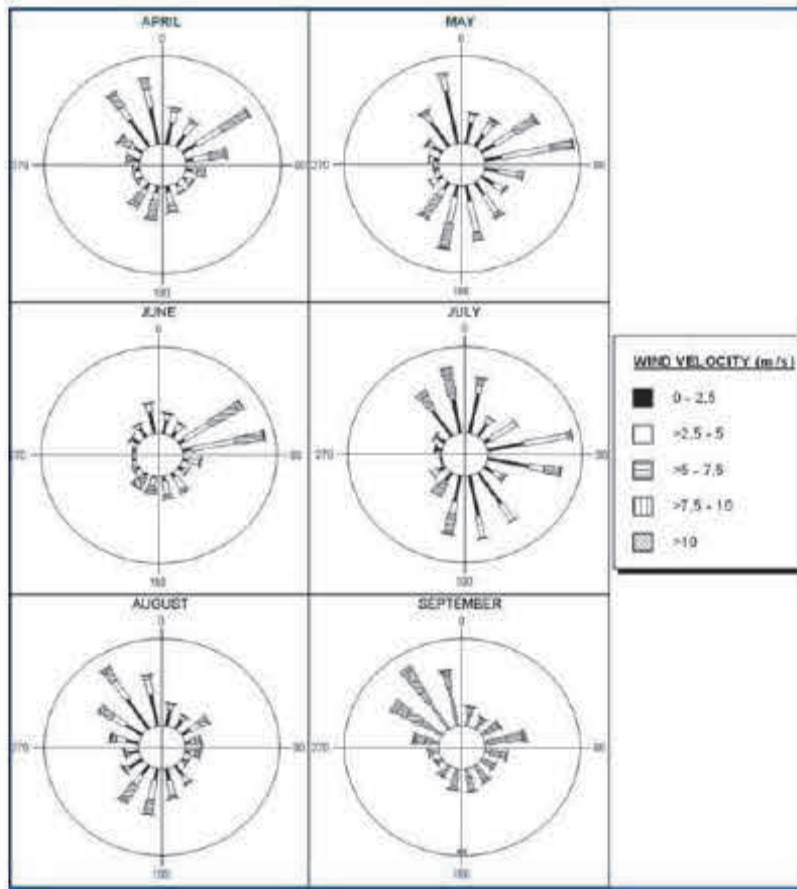


Figure 8

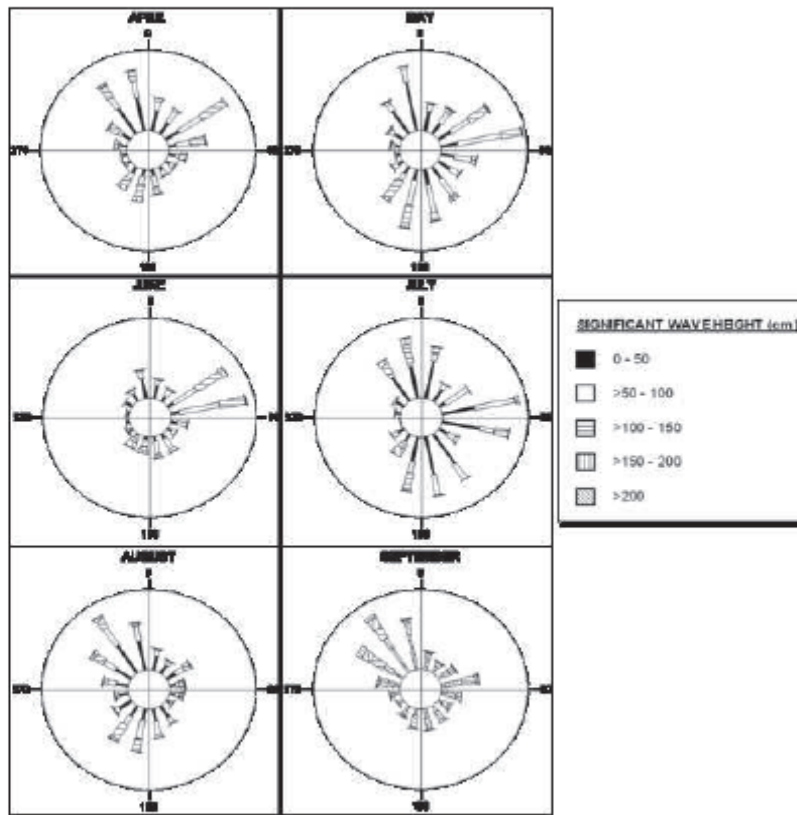
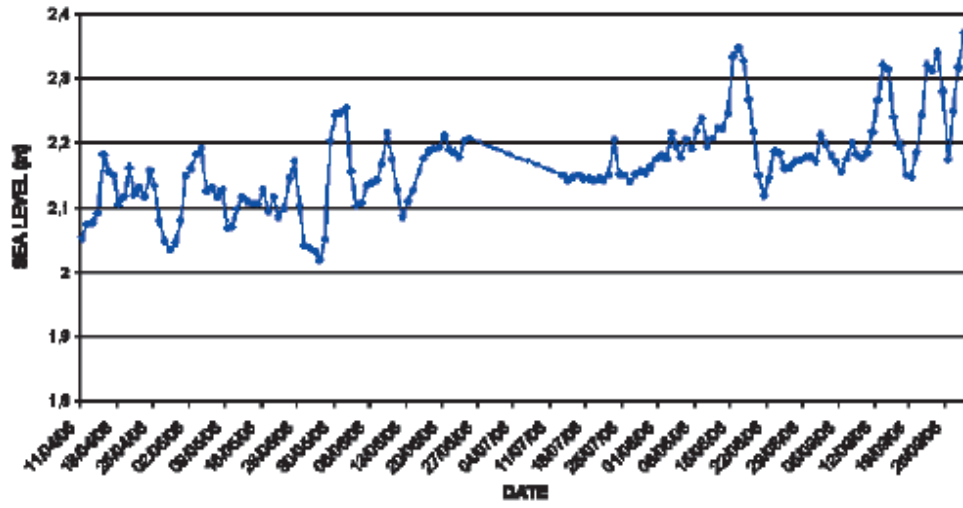
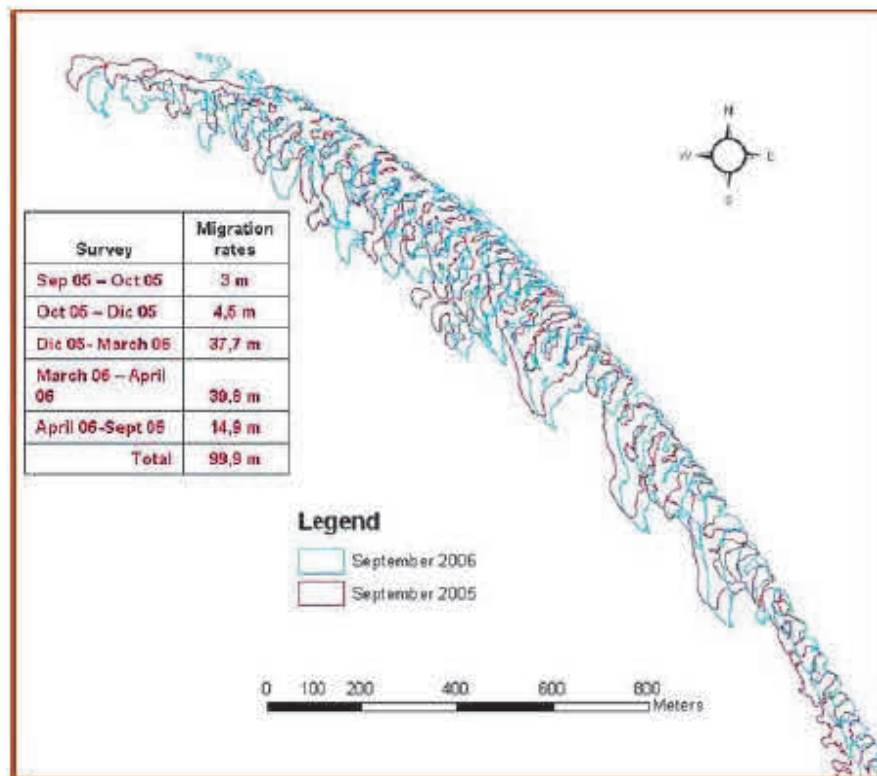


Figure 7



ACCEPTED

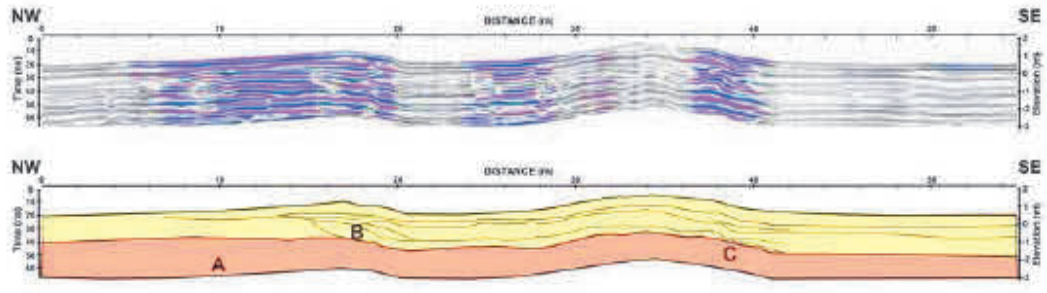
Figure 8



641

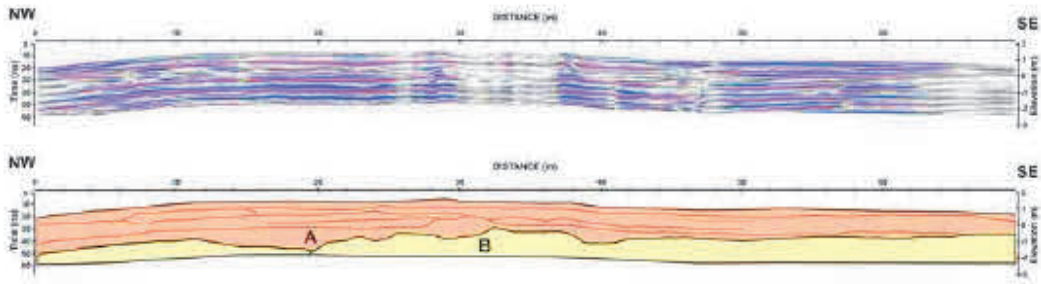
ACCEPTED

Figure 9



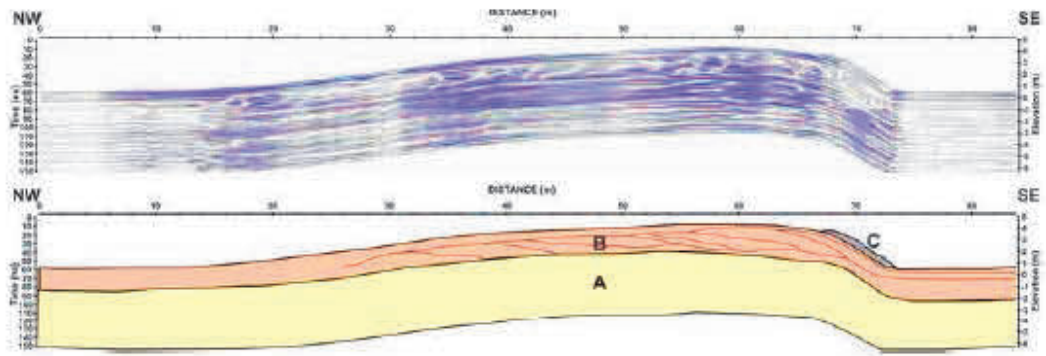
ACCEPTED

Figure 10



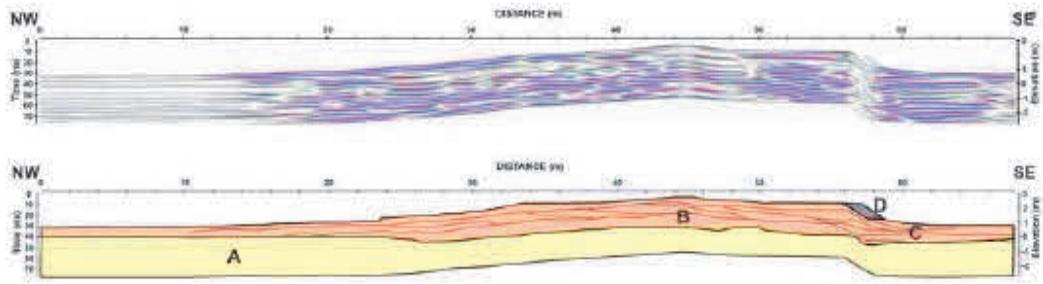
ACCEPTED

Figure 11



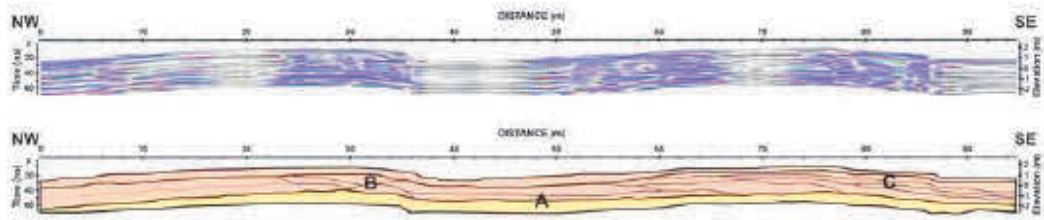
ACCEPTED

Figure 12



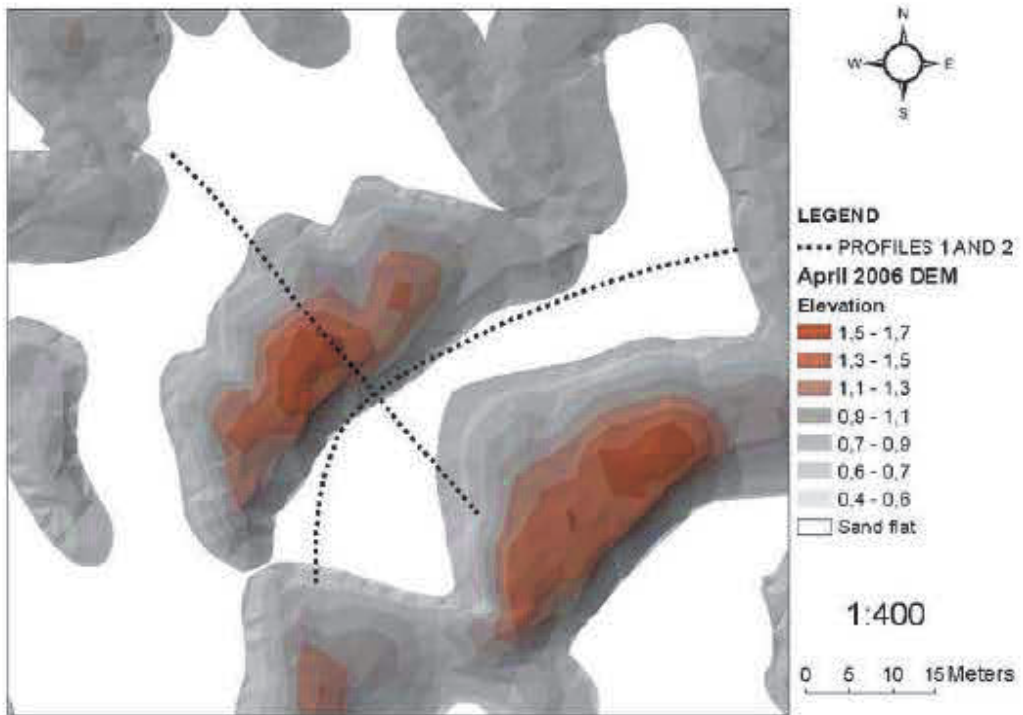
ACCEPTED

Figure 18



ACCEPTED

Figure 14



647

ACCEPTED

Figure 15



ACCEPTÉ

Figure 18



ACCEPTED